MECHANICAL CHARACTERIZATION OF THIN-WALLED GFRP MEMBERS BASED ON EXPERIMENTAL DYNAMIC TESTING

Jessé Beserra
Cássio Gaspar
Daniel Cardoso
jesse.eng@yahoo.com
cassiogaspar@esp.puc-rio.br
dctcardoso@puc-rio.br
Pontifical Catholic University of Rio de Janeiro, Dept. of Civil Engineering
R. Marques de Sao Vicente, 225 – Gavea, 22451-900, Rio de Janeiro, RJ, Brazil

Abstract. The use of composite materials such as pultruded members of glass-fiber reinforced polymer (GFRP) has increased in recent years, with important applications for footbridges, bridge decks, cooling towers, stair towers, industrial structures, and rapid-assembly kits for temporary accommodation. The mechanical characterization of GFRP in terms of elastic properties is often carried out by means of destructive tests as specified by international standards. On the other hand, recent studies have proposed the use of non-destructive techniques based on dynamic testing also known as experimental modal analysis (EMA). In this sense, this work aims to identify the dynamic properties of thin-walled GFRP members regarding their natural frequencies, mode shapes and damping ratios. These experimental dynamic characteristics obtained for a C-channel beam are, then, used to determine specific material elastic properties back-calculated from numerical optimization process. Finally, the properties determined from proposed approach are compared to those obtained from classical destructive tests. Therefore, the non-destructive procedure presented in this paper gives an alternative approach for the mechanical characterization of GFRP members, which is especially important for low cost in situ quality control.

Keywords: Glass-fiber reinforced polymer, dynamic testing, dynamic properties, experimental modal analysis, mechanical characterization.

1 Introduction

Worldwide structural systems are mostly designed by architects and engineers in traditional materials, either by using steel, concrete, both steel-concrete and even wood. On the other hand, the use of composite fiber-reinforced polymer (FRP) materials has increased in recent years, with important applications for cooling towers, stair towers, pedestrian bridges, bridge decks, industrial sheds, building façades and restoration of historic structures (Bakis et al. [1], Jacob [2], Russo [3]).

The main mechanical properties of GFRP are related to its high corrosion resistance, high strength (similar to steel) and strength/weight ratio, relatively low specific weight – which results in reduced costs associated with transportation, assembly and maintenance –, low thermal conductivity, electromagnetic transparency, and low energy consumption in production (for the benefit of the environmental impact). These advantages would make the use of GRFP as a major competitor over traditional building materials.

Regarding the vibration tests of structural systems designed in GFRP, several studies have characterized their dynamic parameters (natural frequencies, vibration modes and damping) through experimental modal analysis (EMA) techniques (Russo [3]; Gonilha et al. [4]; Ahmadi et al. [5]) and operational modal analysis (OMA) (Wei et al. [6], [7]). It should be noted that these dynamic tests are equally important for calibrating numerical and analytical models via non-destructively techniques (Russo [3], Gonilha et al. [4]).

Besides, compared to conventional materials (steel-concrete), structures made of GFRP are even lighter, making them more susceptible to excessive vibration problems (Ascione et al. [8]; Gonilha et al. [4], Ahmadi et al. [5]). Additionally, the low damping ratio of these composite materials - which has an average value of 1.5% - contributes to this issue. Even though some authors have reported values damping ratios below 1% for GFRP structures (Song et al. [9]; Ahmadi et al. [5]).

Therefore, considering all the aspects mentioned above, the main motivation of this paper is to determine experimentally the longitudinal and shear modulus of GFRP C-channel profiles through traditional destructive tests (i) and based on non-destructive tests by means of dynamic modal testing (ii). After that, the elastic properties obtained by both procedures are compared and discussed.

2 Mechanical characterization of GFRP coupons based on destructive tests

2.1 Tests procedure

The experimental tests were carried out at Pontifical Catholic University of Rio de Janeiro (PUC-Rio). Firstly, it is important to show the geometric properties from the pultruded GFRP beam that was used for this work. The C-channel beam profile has a vinyl ester matrix and was fabricated by "Cogumelo Brasil". Fig. 1 illustrates the cross-section of the investigated beam. Also, it must be said that the major part of the destructive test specimens was taken from a similar profile to those tested in dynamic tests. The two profiles have the same fiber reinforcement, matrix and geometry.

The universal testing machine used for tensile (Fig. 2b) test has a load capacitive of 1200kN and 103.4MPa (15000psi) of pressure on the grips, whilst the equipment used for compressive and shear tests has capacity for 500kN of load (see Fig. 2a, c and d). In order to determine the tensile properties of the GFRP beam, four specimens were prepared: two obtained of them from the flange and the other ones from the web. Each specimen had two pairs of aluminum tabs (1.5mm width) bonded at their ends, aiming to prevent any type of crushing on the interface with the equipment grips and, thus, causing sliding. All four specimens had same geometric properties, based on specimens type 2 preconized by ISO 527-4 [10], as shown in Fig. 3a and b. Also, all specimens were tested at a grip pressure of 5.15MPa (800psi) what is enough to perform the tests and not crush the specimen ends. The tests were conducted at a displacement rate of 0.5mm/min and did not have measurements by strain gages on the specimen, but rather were acquired from a clip gage installed on half-length from the grips (see Fig. 2b).

a) Isometric view

b) Cross-section dimensions (mm)
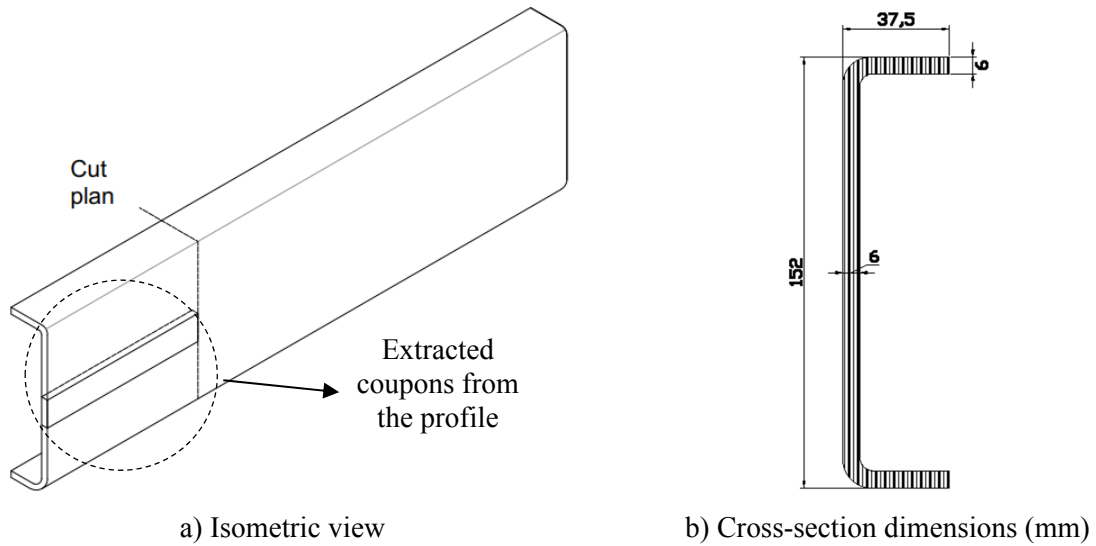
Figure 1. Geometric properties of the investigated GFRP C-channel profiles
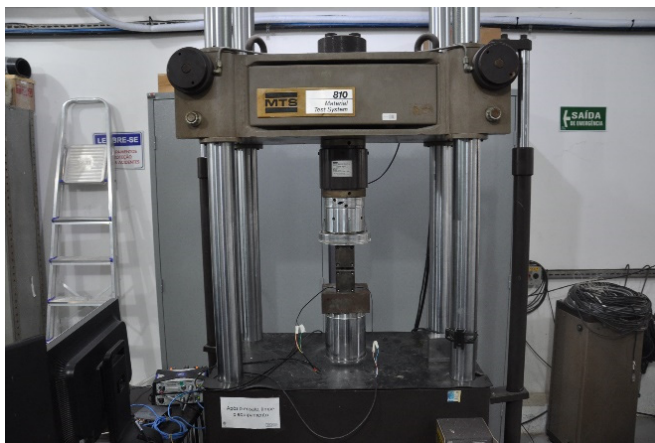
a) Universal testing machine (MTS 810/500) for compressive and shear tests

b) Tensile tests
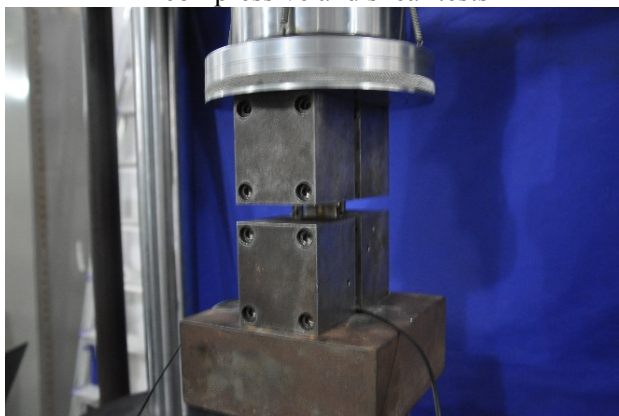
c) Compressive tests
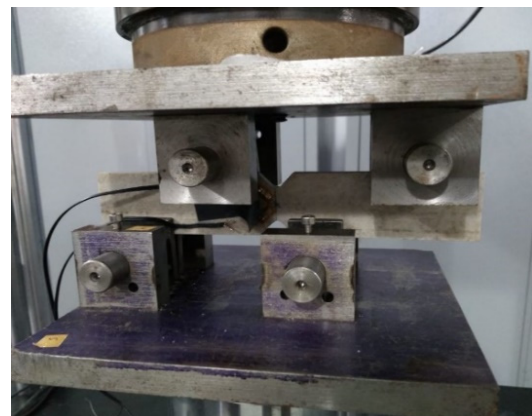
d) Shear tests

Figure 2. Overview of the destructive tests
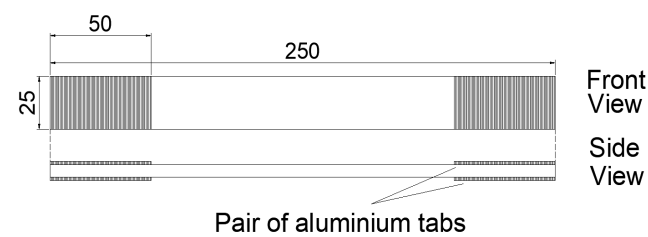
a) Typical tensile test specimen dimensions (mm)

b) Tensile test specimens
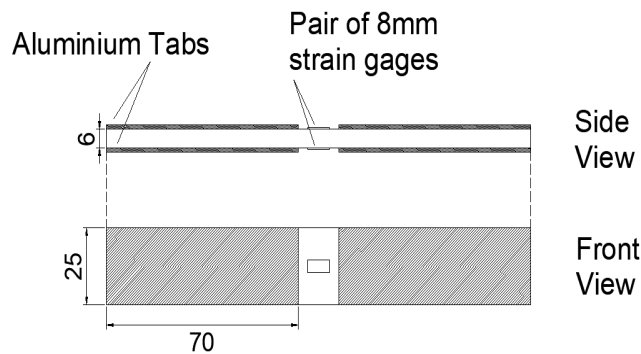
c) Typical tensile test specimen dimensions (mm)

d) Compressive test specimens
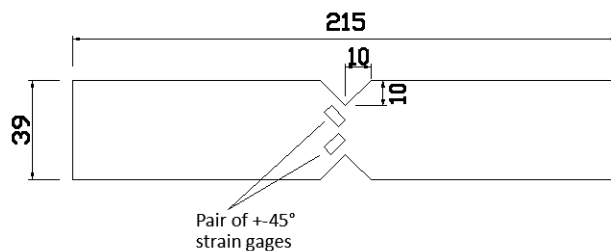
e) Typical shear test specimen dimensions (mm)

f) Shear test specimens

Figure 3. Preparation of GRFP specimens for destructive tests

To obtain the compressive resistance, three different specimen sizes were designed to be used in the Compressive Load Compression (CLC) tests. These three sizes were intended to evaluate the influence of buckling and barreling effects along unsupported length and, thus, on modulus results. As suggested by ASTM D6641 [11], a pair of strain gages (8mm in this work) were positioned on each face of the specimens, as shown in Fig. 3 c and d, aiming at detecting any buckling effect. All specimens received two pairs of aluminum tabs on the contact surface with the CLC setup (Fig. 4a), trying to avoid any end crushing on testing and to prevent damages due to torque application at the CLC bolts. The displacement rate used on these tests were 0.5mm/min and all specimens were tested with 11N.m torque at each CLC setup bolt. It is important to point out that the screw tightening must be done gently, trying to maintain the setup alignment as perfect as possible. Also, the specimen ends must be in perfect alignment with the setup surface in contact with the applied load. These two mistakes are extremely common and can lead to major mistakes on modulus results.

The shear test done is an adaptation from the test proposed by ASTM D5379 (Iosipescu) [12] and had the intention to measure the shear modulus. Three specimens of 215 mm x 39 mm were prepared with two V nodes of 10mm on each side (see Fig. 3e and f) and tested as illustrated in Fig. 4b.

a) Compressive load compression (CLC) setup   b) ASTM D5379 Iosipescu shear test
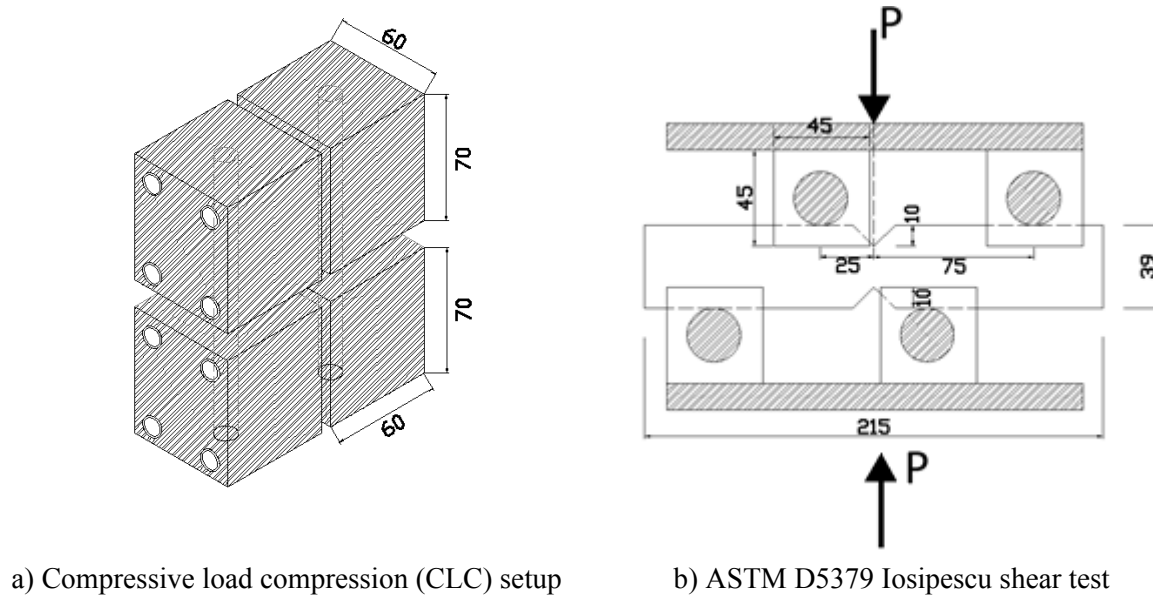
Figure 4. Compressive and shear tests scheme (dimensions in mm)

2.2 Elastic properties determination of the selected GFRP coupons

To properly calculate the elastic properties, it is important to plot the stress x strain diagrams to identify each specimen behavior. Afterwards, the longitudinal compressive and tensile modulus as well as the shear modulus were obtained based on classical equations derived from Mechanics of Materials [13].

Table 1 presents the longitudinal compressive, $E_{L,c}$ (GPa) and tensile modulus, $E_{L,t}$ (GPa) obtained from the experimental tests whilst Fig. 5 depicts the stress x strain plots. Global mean ± standard values deviation of $E_{L,c}$ and $E_{L,t}$ were equal to 28.96 ± 2.69 GPa and 26.03 ± 4.17 GPa, respectively. It should be noted that the mean values lie in the range reported in literature [14], varying from 16.8 to 30.7 GPa ($E_{L,c}$) and from 17.4 to 28.3 GPa ($E_{L,t}$). Regarding the compressive moduli ($E_{L,c}$), it was verified that major part of specimens presents different modulus results between the strain gages, which can be caused by not perfect symmetrical strain gage positioning on each side of the specimens and due to buckling effects. On the other hand, tensile tests generated only one modulus result per specimen, which show higher values on specimens taken from the flange.

Concerning the shear test results in Table 2, the shear modulus presented a global mean ± standard deviation value equal to 4.90 ±1.71 GPa. The mean value is found in literature range from 2.4 to 5.7 GPa. Fig. 6 shows the typical shear stress-strain curves. The non-linear behavior of the curves agrees with Zureick [15]. It is important to point out that the specimen S-03 had a test problem. There was a programming mistake that led to extremely high load rate, making the specimen fail within 30 seconds. This can justify the high difference between the modulus for this specimen and the others. However, this value (2.95 GPa) still lies in literature range [14]. Fig. 7 depicts the typical failure patterns of specimens from all destructive tests.

Table 1. Experimental longitudinal compressive ($E_{L,c}$) and tensile modulus ($E_{L,t}$)

Specimen reference (SPEC-CXXX-YY)	Longitudinal compressive modulus, $E_{L,c}$ (GPa)		Global mean ± standard deviation (GPa)
	Strain gage 01	Strain gage 02	
SPEC-C155-01	29.80	25.57	
SPEC-C155-02	27.95	33.18	
SPEC-C155-03	29.62	25.69	
SPEC-C155-04	25.06	30.07	
SPEC-C165-01	34.25	28.35	28.96 ± 2.69
SPEC-C165-02	25.93	32.65	
SPEC-C165-03	25.51	28.65	
SPEC-C175-01	26.89	31.41	
SPEC-C175-02	30.99	28.20	
SPEC-C175-03	29.58	29.76	
Specimen reference	Longitudinal tensile modulus, $E_{L,t}$ (GPa)		Global mean ± standard deviation (GPa)
SPEC -T-W-01	25.0		
SPEC -T-W-02	21.7		26.03 ± 4.17
SPEC -T-F-01	31.7		
SPEC -T-F-02	25.7		

Notes: "C", "T", "XXX" and "YY" indicate "compressive test", "tensile test", the coupon length (mm) and the specimen number, respectively. "W" and "F" mean that the corresponding coupon was extracted from the "web" and the "flange" of the GFRP C-channel profile.

a) Tensile tests   b) Compressive tests (SPEC-C155-03)
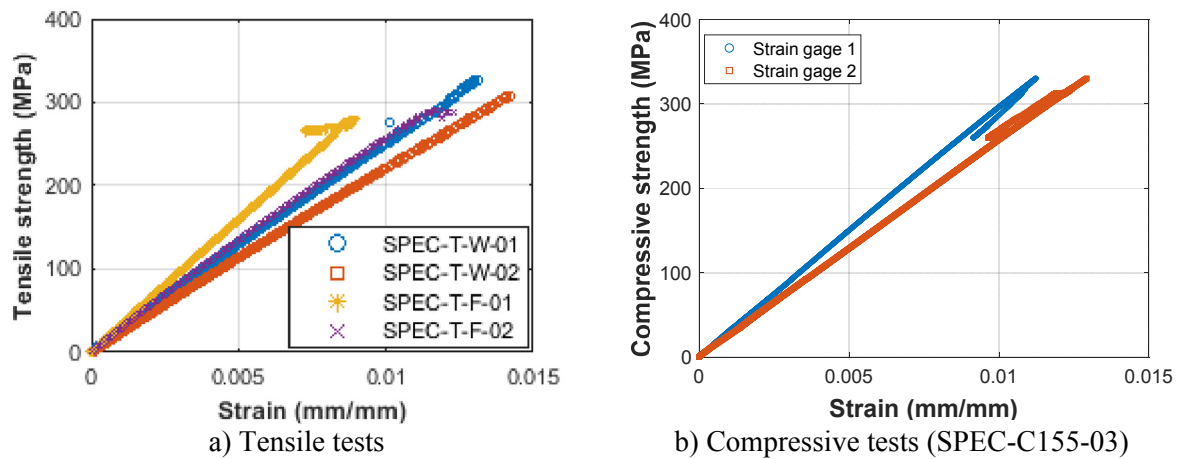
Figure 5. Tensile and compressive stress vs. strain of coupons

Table 2. Experimental shear strain (γ), strength (F_ν) and modulus (G_{LT})

Specimen reference	Shear Strain, γ (rad)	Shear Strength, F_ν (MPa)	Shear modulus, G_{LT} (GPa)	Global mean ± standard deviation (GPa)
SPEC-S-01	0.0070073	43.08	6.15	
SPEC -S-02	0.0070059	39.33	5.61	4.90 ±1.71
SPEC -S-03	0.00717	21.15	2.95	

Note: "S" indicates "shear test".
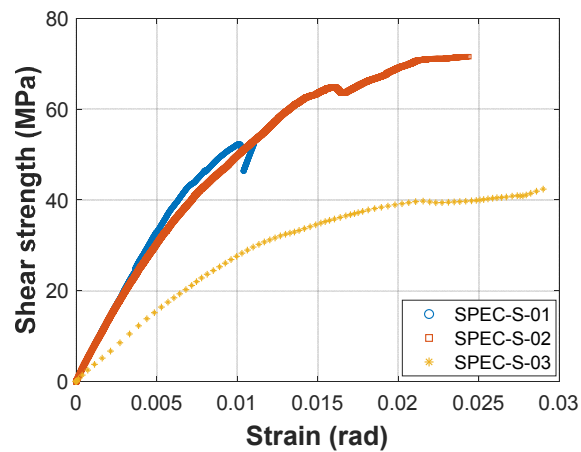
Figure 6. Shear stress vs. strain of coupons

a) Tensile tests

b) Compressive tests

c) Shear tests
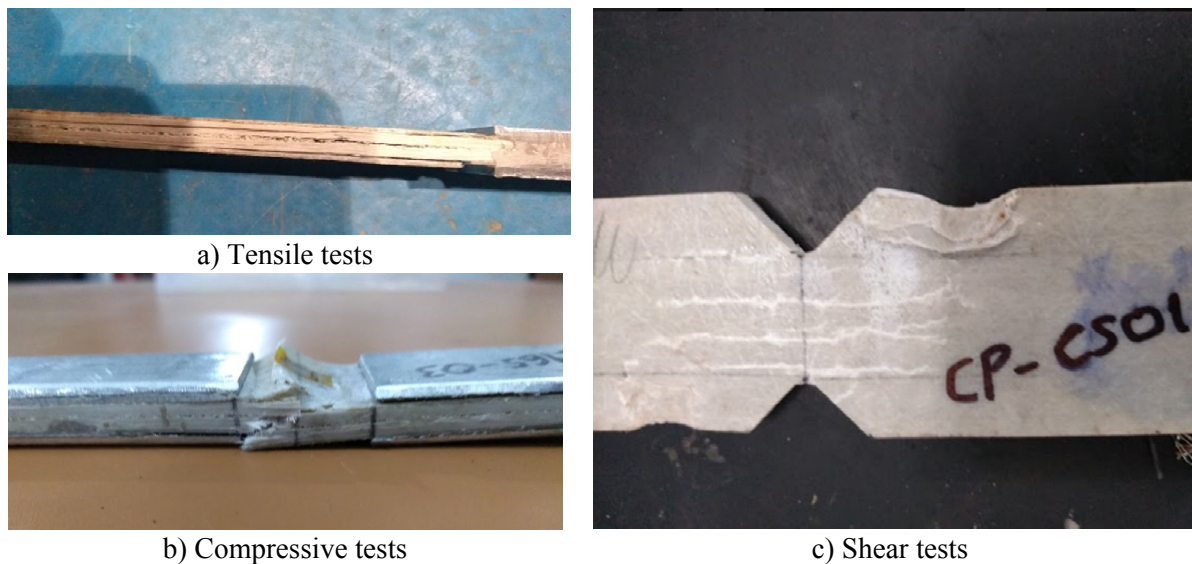
Figure 7. Failure patterns of specimens from destructive tests

3   Dynamic properties identification of the investigated GFRP C-channel beam

3.1 Non-destructive test setup

The investigated C-Channel beam (152 mm x 37.5 mm x 6 mm) spans 2.75 m and is supported at both ends over rollers. Lateral support was also used at ends to prevent warping and lateral motions, as shown in Fig. 8a. It should be noted that this boundary condition approaches the theoretical (idealized) clamped-clamped support. The non-destructive test was carried out based on the well-established impulse technique [16]. It should be noted that this technique is also referred as Experimental Modal Analysis (EMA) [17]. In a nutshell, the main goal of such test is to characterize the dynamic properties of a structure in terms of its natural frequencies, vibration modes and damping ratios.

a) Overview of the investigated GFRP C-channel beam

b) Impact test (free vibration)

c) Data acquisition system
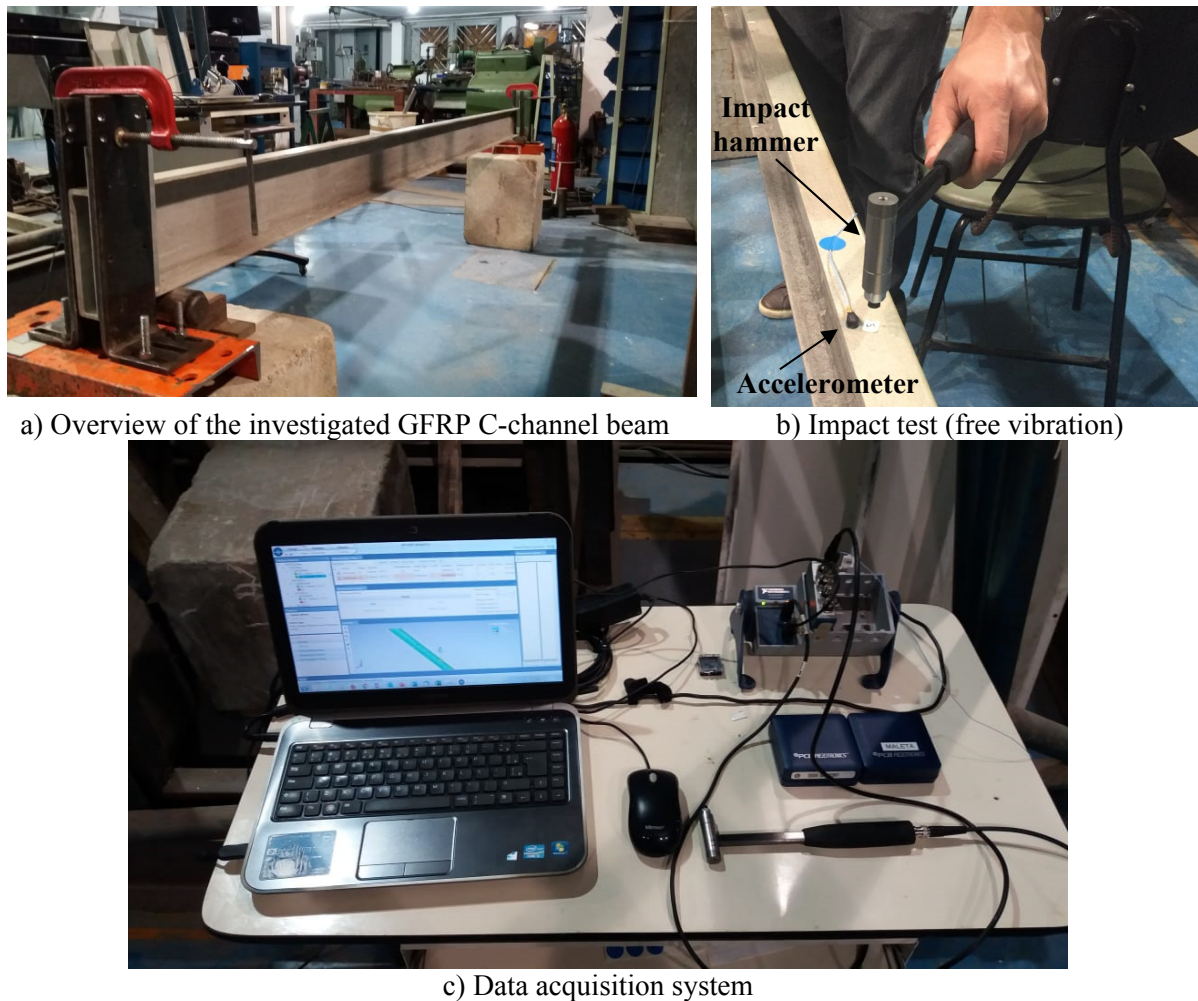
Figure 8. Experimental modal analysis setup

For that, a dynamic force must be applied onto the structural system in such way the structure is able to freely vibrate. This is usually done by an impact hammer which has a piezoelectric force sensor inside its head. On the other hand, the impulse excitation induced by the hammer is commonly measured by appropriate accelerometers, as depicted in Fig. 8b. The signals from the hammer and the uniaxial accelerometer used herein (types PCB Piezotronics 086C03 and 352A24, respectively) were acquired through the cDAQ-9174 acquisition system from National Instruments (NI), equipped with Integrated Electronic Piezoelectric (IEPE) analogue input modules (NI 9233), as seen in Fig. 8c.

3.2 Experimental modal analysis and numerical model updating

Before starting the tests, it is important to have an idea (whenever it is possible) about the expected dynamic behavior of the structure. As the cross-section of the C-channel beam is an open section and has only one axis of symmetry, the centroid and the shear center about major moment of inertia axis do not coincide. Thus, the transversal bending and torsional vibrations are coupled (Rao [18]).

In this sense, a numerical model was implemented in the ANSYS program [19] considering the usual mesh refinement techniques present in finite element method simulations. In this computational model, the GFRP beam was represented by shell finite elements (SHELL181), which is well-suited for analyzing thin to moderately-thick shell structures and allows the simulation of the material orthotropic behavior, as shown in Fig. 9a and b. Afterwards, the beam natural frequencies and vibration modes were determined with the aid of the numerical extraction methods (modal analysis) in order to identify the first three flexural-torsional vibration modes [19].
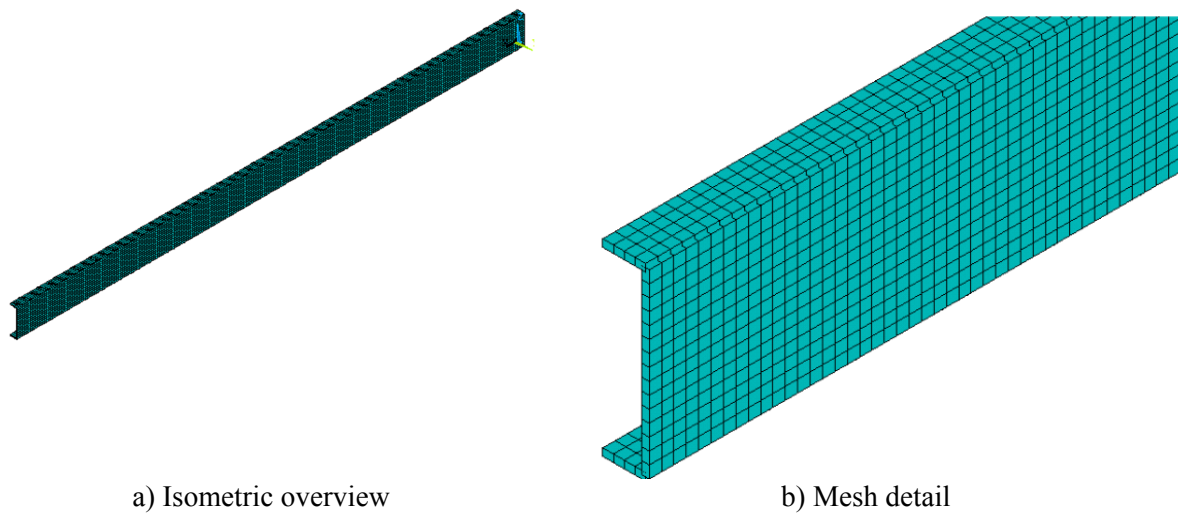
|a) Isometric overview|b) Mesh detail|

Figure 9. GFRP C-channel beam numerical model (ANSYS [19])
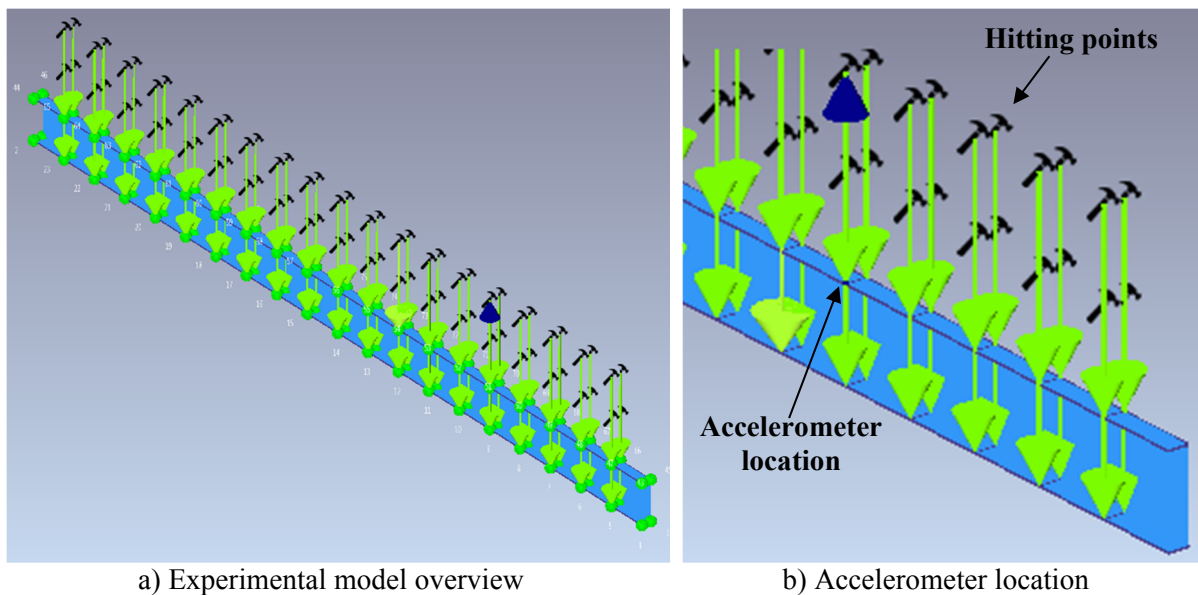
|a) Experimental model overview|b) Accelerometer location|

Figure 10. GFRP C-channel beam experimental model (ARTeMIS [22])

With respect to the experimental model, the determination of how many points should be excited by the hammer is not a simple task. The key aspect is that there must be enough measurement points to see the waveform of the desirable experimental mode shapes (Avitabile [20]). Since GRFP is a composite material, it is prudent to test many points along the beam. Therefore, the beam was divided into 20 equally spaced segments. The impact test was performed on the four-corner points of 19 sections (excluding the supports), which gives a total of 76 impact points in vertical direction. In turn, each point was hit 3 times to obtain average values for signal processing purposes (Brandt [21]). Fig. 10 shows the location of the impact points as well as the reference accelerometer position. It is worth emphasizing that the accelerometer should be placed (whenever it is possible) where there is a common antinode among the mode shapes of interest. Otherwise, if the accelerometer is positioned at a node of a mode shape, will note capture a desirable vibration mode.

a) Force impact (driving point)

b) Acceleration response (driving point)

c) Complex mode indicator function (CMIF) - frequency domain
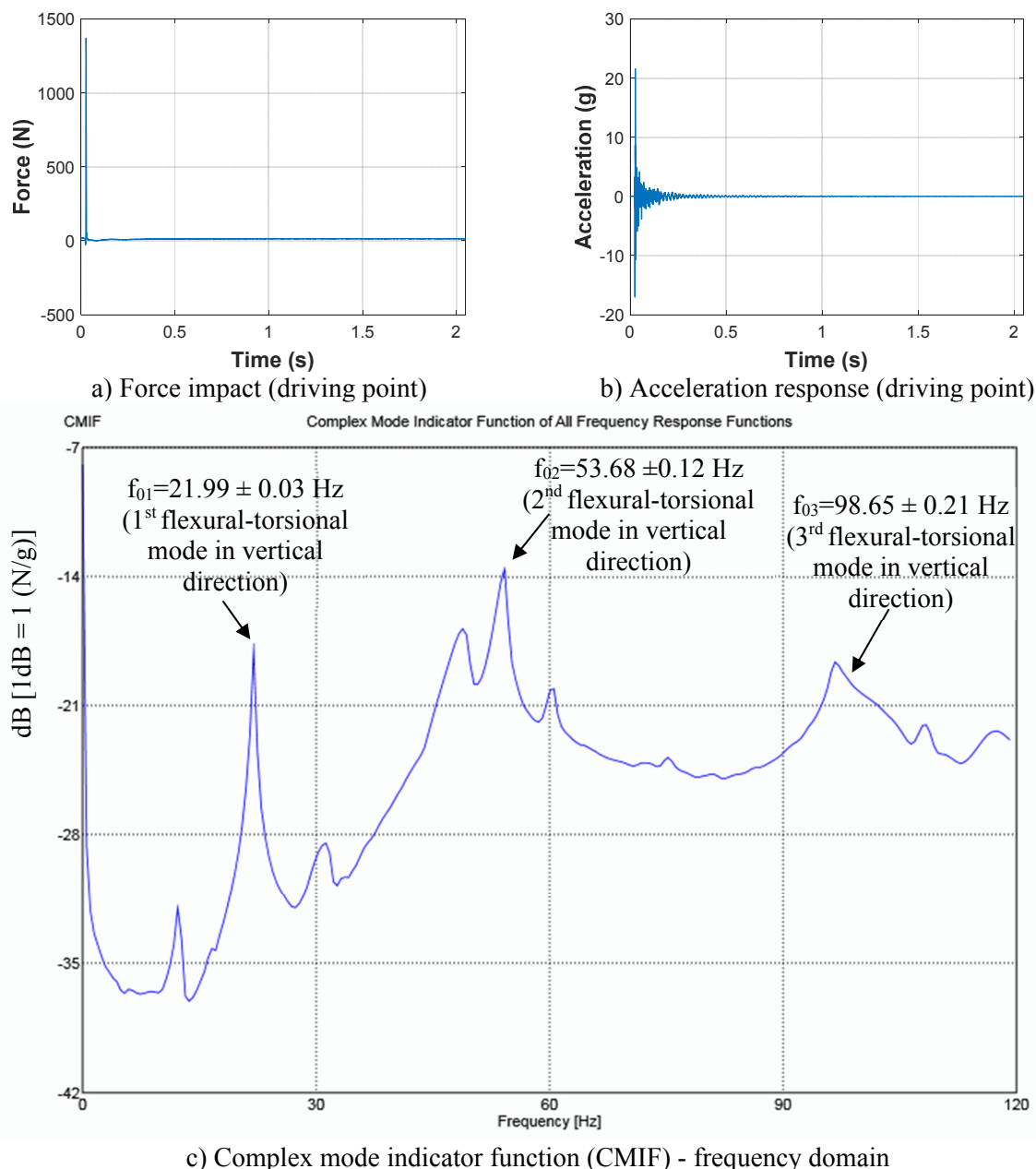
Figure 11. Experimental modal analysis response in time and frequency domain (ARTeMIS [22])

The tests were performed and processed in ARTeMIS program [22]. The signals were recorded with a sampling frequency of 2000 Hz which is enough to capture natural frequencies until 1000 Hz according to the sampling theorem (Brandt [21]). Fig. 11a and b shows an example, in time domain, of the input force signal of the hammer and the output acceleration signal of the accelerometer at the driving point, i.e. where the impact and the response occur at the same location. On the other hand, the dynamic behavior of the structure is often evaluated in frequency domain. Thus, the relationship between the output and input signals, in frequency domain, is defined as the Frequency Response Function (FRF) of the system (Avitabile [20], Brandt [21], Ewins [23]). In order to compute the 76 experimental average FRFs in one plot, the Complex Mode Indicator Function (CMIF) was used. The CMIF is helpful to determine all the principal modes that are observed in the set of measurements (Avitabile [20]). Besides, the Rational Fraction Polynomial in Z domain method (RFP-Z) was used to identify the first three flexural-torsional modes in vertical direction [22]. Fig. 11c reveals, in frequency domain, the identified experimental natural frequencies whereas Fig. 12 shows a comparison between the experimental and numerical vibration modes.

a) 1st flexural-torsional experimental mode   b) 1st flexural-torsional numerical mode

c) 2nd flexural-torsional experimental mode   d) 2nd flexural-torsional numerical mode

e) 3rd flexural-torsional experimental mode   f) 3rd flexural-torsional numerical mode
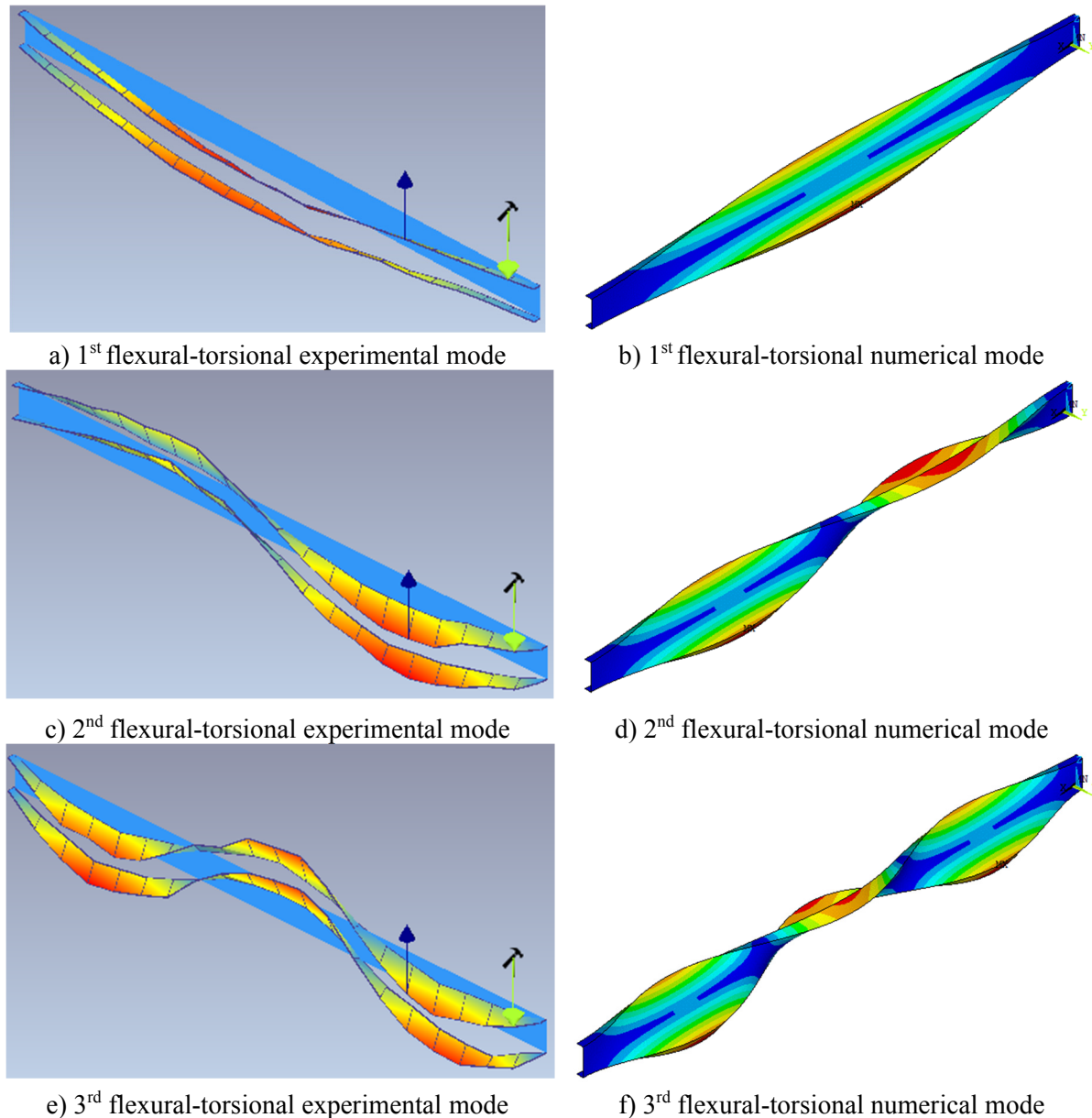
Figure 12. Vibration modes of the experimental and numerical model in vertical direction

From Fig. 12 it can be seen a good agreement between the experimental and numerical shapes, which means that a relationship between both models can be established. Therefore, the elastic properties of the GRFP C-channel beam can be found through model updating techniques based on optimization processes (Tam et al. [16]). Considering the Subproblem Approximation Method (Rao [24], Vanderplaats [25], Gaspar et al. [26]) available in Ansys program [19], an optimization problem can be defined in terms of design variables (DV) and state variables (SV). The objective function to be minimized is obtained by summing the relative errors between the numerical and the experimental natural frequencies [27].

Table 4 presents the design variables (DV) of the optimization problem. This way, the longitudinal E_L (GPa) and the shear modulus G_{LT} (GPa) are set up as design variables. The lower and upper bound limits of these variables are chosen in accordance with the experimental values present in Tables 1 and 2. The first design values of E_L (26.03 GPa) and G_{LT} (4.90 GPa) were attributed as the mean values of the compressive tests and shear tests, respectively. Although the major (ν_{LT}) and minor (ν_{TL}) Poisson's ratios were not obtained experimentally herein, the bound limits was set up according to the values found in literature (Cardoso [14]).

It should be noted that since GRFP is an orthotropic material, a relationship between the longitudinal and transversal moduli is established in function of the major and minor Poisson's ratios. With respect to the state variables, they are the first three natural frequencies of interest with a tolerance of ± 2% in relation to the experimental ones. The state variables constraints the optimization problem in order to find feasible values. The optimal design of E_L and G_{LT} are equal to 28.29 GPa and 2.96 GPa, respectively.

Table 4. Design and state variables of the optimization problem

Variable Type	Variables	Bound Limits		First design	Optimal design
		Lower	Upper		
Design variables	E_L (GPa)	21.70	34.25	26.03	28.29
	G_{LT} (GPa)	2.95	6.15	4.90	2.96
	Major Poisson's ratio (ν_{LT})	0.280	0.350	0.280	0.296
	Minor Poisson's ratio (ν_{TL})	0.150	0.170	0.170	0.152

Table 5 presents a comparison between the natural frequencies of the numerical and experimental models. It is interesting to note a significant decrease (e.g. from 16.85% to 1.83% - 1st vibration mode) in the relative error between the numerical and experimental values for the three vibration modes when the optimization problem is considered. These results indicate that a good calibration between the models was reached. It can also be seen in Table 5 the experimental damping ratio (%) values of 0.84 ± 0.35, 1.38 ±0.56 and 2.78 ± 0.31 corresponding to the first three vibration modes. These values are in line with the expected ones for FRP materials (Ascione [8]).

Table 5. Comparison between the experimental and numerical frequencies

Mode	Experimental model (RFP-Z method)		Numerical model			
			First design		Optimal design	
	Frequency (Hz)	Damping ratio (%)	Frequency (Hz)	Δ* (%)	Frequency (Hz)	Δ* (%)
1	21.99 ± 0.03	0.84 ± 0.35	25.70	16.85	22.40	1.83
2	53.68 ±0.12	1.38 ±0.56	59.43	10.71	53.61	0.13
3	98.65 ± 0.21	2.78 ± 0.31	104.81	6.24	96.73	1.98

*Relative error between the numerical and experimental values [(numerical-experimental)/experimental]

4   Conclusions

The use of composite glass-fiber reinforced polymer (GFRP) materials has increased in recent years. Although the main advantages of this orthotropic material are mainly related to high corrosion resistance, high strength/weight ratio and relatively low specific weight, the intrinsic low longitudinal modulus of elasticity of GRFP may lead slender structural systems to buckling problems. Therefore, to better understand the material behavior, this work evaluated experimentally - through traditional destructive tests - the longitudinal compressive and tensile moduli as well as the shear modulus of a GRFP C-channel beam. The mean values were equal to 28.96 ± 2.69 GPa, 26.03 ± 4.17 GPa and 4.90 ±1.71 GPa, respectively.

Second, an impact test by means of non-destructive techniques was performed on a clamped-clamped GRFP C-Channel beam spanning 2.75 m with cross-section dimensions of 152 mm x 37.5 mm x 6 mm. The first three experimental natural frequencies in vertical direction were equal to 21.99 ± 0.03 Hz, 53.68 ±0.12 Hz and 98.65 ± 0.21 Hz, respectively. Finally, in order to back-calculate the elastic properties of the investigated GRFP beam, a numerical updating model based on finite element method (FEM) and optimization process was carried out. The optimal longitudinal modulus of elasticity and

shear modulus were equal to 28.29 GPa and 2.96 GPa, respectively. The relative error between the numerical and experimental natural frequencies was set to be within ± 2% which presented a good calibration between both models. Besides, the calibrated values regarding the longitudinal and shear modulus are within the limits expected in literature. Therefore, the non-destructive procedure presented in this work offers an alternative approach for the mechanical characterization of GFRP members, which is especially important for low cost in situ quality control.

Acknowledgements

References

[1]   C. Bakis et al. Fiber-reinforced polymer composites for construction-state-of-the-art review. *Journal of Composites for Construction*, vol. 6, n.2, pp. 73–87, 2002.

[2]   A. Jacob. Globalisation of the pultrusion industry. *Reinforced Plastics*, vol.50, n. 5, pp. 38–41, 2006.

[3]   S. Russo. Experimental and finite element analysis of a very large pultruded FRP structure subjected to free vibration. Composite structures, vol. 94, n. 3, pp. 1097–1105, 2012.

[4]   J.A. Gonilha et al. Modal identification of a GFRP-concrete hybrid footbridge prototype: Experimental tests and analytical and numerical simulations. Composite Structures, vol. 106, pp. 724–733, 2013.

[5]   E. Ahmadi et al. Vertical ground reaction forces on rigid and vibrating surfaces for vibration serviceability assessment of structures. Engineering Structures, vol. 172, n. February, pp. 723–738, 2018.

[6]   X. Wei et al. Experimental Investigation of the Dynamic Characteristics of a Glass-FRP Suspension Footbridge. In: J. Caicedo, S. Pakzad (ed.), Dynamics of Civil Structures, Volume 2. Conference Proceedings of the Society for Experimental Mechanics Series. Springer, 2017.

[7]   X. Wei et al. Experimental Characterisation of Dynamic Properties of an All-FRP Truss Bridge. In: S. Pakzad (ed.), Dynamics of Civil Structures, Volume 2. Conference Proceedings of the Society for Experimental Mechanics Series. Springer, 2018.

[8]   L. Ascione et al. Prospect for new guidance in the design of FRP. EUR 27666 EN; 2016.

[9]   G. Song et al. Active vibration control of a smart pultruded fiber-reinforced polymer I-beam. Smart Materials and Structures, vol. 13, n. 4, pp. 819–827, 2004.

[10] ISO 527-4. Plastics - Determination of tensile properties - Part 4: Test conditions for isotropic and orthotropic fibre-reinforced plastic composites, 1997.

[11] ASTM Standard D6641/D6641M-09. Determining the compressive properties of polymer matrix composite laminates using a combined loading compression (CLC) test fixture, ASTM International, West Conshohocken, PA, 2009.

[12] ASTM Standard D5379/D5379M-12. "Test method for shear properties of composite materials by the V-notched beam method", ASTM International, West Conshohocken, PA, 2012.

[13] R.C. Hibbeler. Mechanics of Materials. Fifth Edition, 2002.

[14] D.C.T. Cardoso. Compressive strength of pultruded glass-fiber reinforced polymer (GFRP) columns. D.Sc. thesis, COPPE - Federal University of Rio de Janeiro, Rio de Janeiro, Brazil, 2014.

[15] A. Zureick, R. Steffen. Behavior and design of concentrically loaded pultruded angle struts. ASCE Journal of Structural Engineering, vol. 126, n. 3, pp. 406–416, 2000.

[16] J.H. Tam, Z.C. Ong, Z. Ismail, B.C. Ang and S. Y. Khoo. Identification of material properties of composite materials using nondestructive vibrational evaluation approaches: A review. Mechanics of Advanced Materials and Structures, vol. 24, n.12, pp. 971–986, 2017.

[17] A. Cunha, E. Caetano. Experimental Modal Analysis of Civil Engineering Structures. *Sound and Vibration*, vol. 40, pp. 12–20, 2006.

[18] S.S. Rao. Vibration of Continuous Systems. Fourth Edition, John Wiley & Sons, 2019.

[19] ANSYS Swanson Analysis Systems, version 12.1, 2009.

[20] P. Avitabile. Modal Testing: A practitioner's guide. First Edition, John Wiley & Sons, 2018.

[21] A. Brandt. Noise and Vibration Analysis: Signal Analysis and Experimental Procedures, First Edition, John Wiley & Sons, 2011.

[22] Structural-Vibration-Solutions, ARTeMIS Modal Pro 6.0, 2019.

[23] D.J. Ewins. Modal Testing: Theory, Practice and Application. Second Edition, John Wiley & Sons, 2000.

[24] S.S. Rao. Engineering Optimization: Theory and Practice, Fourth Edition, John Wiley & Sons, 2009.

[25] G.N. Vanderplaats. Numerical Optimization Techniques for Engineering Design. McGraw Hill, 1984.

[26] C.M.R. Gaspar, J. G. S. Silva, F. J. C. P. Soeiro, L. F. C. Neves. Vibration Control of Building Steel-Concrete Composite Floors Submitted to Aerobics Based on Optimization Techniques. In: The Twelfth International Conference on Computational Structures Technology (CST2014), 2014.

[27] D.D. Vaz, G. Ferreira, D. Ribeiro, R. Calçada. Experimental calibration of a railway bridge dynamic model. In: calibração experimental de um modelo dinâmico de uma ponte ferroviária, Porto, Portugal, 2019.